Geochemistry Geophysics Geosystems G3
AN ELECTRONIC JOURNAL OF THE EARTH SCIENCES
Published by AGU and the Geochemical Society

Article
Volume 5, Number 8
25 August 2004
Q08011, doi:10.1029/2004GC000719
ISSN: 1525-2027

Geothermal fluxes of alkalinity in the Narayani river system of central Nepal

Matthew J. Evans
Chemical Sciences Division, Oak Ridge National Laboratory, P.O. Box 2008, MS 6375, Oak Ridge, Tennessee 37831, USA (evansmj@ornl.gov)

Louis A. Derry
Department of Earth and Atmospheric Sciences, Cornell University, Ithaca, New York 14853, USA (lad9@cornell.edu)

Christian France-Lanord
Centre de Recherches Pétrographiques et Géochimiques/CNRS, BP20 54501 Vandœuvre les Nancy, France (cfl@crpg.cnrs-nancy.fr)

[1] Numerous hot springs flow within the steeply incised gorges of the central Nepal Himalayan front. The spring fluids have total dissolved solids (TDS) up to 7000 mg/L and Na^+, and K^+ typically comprise >50% of the cationic charge, indicating that high-temperature silicate alteration is the dominant source of hot spring alkalinity. HCO_3^- is normally the dominant anion. Sr isotope ratios from the hydrothermal fluids are similar to the range of values found in the host rocks and imply significant fluid-rock interaction with local lithologies. To determine the impact of the hydrothermal solute load on the local and regional river chemistry, we use a chemical mass balance approach to quantify the hot spring discharge. The springs are ubiquitously enriched in germanium (Ge) with high but variable Ge/Si. Himalayan rivers upstream of the hot spring zones have Ge/Si systematics like other unpolluted rivers, but downstream they are highly anomalous, with Ge/Si from 2 to 20 μmol/mol. Ge and Si appear to behave conservatively during mixing of spring and river, and the large disparity between river and spring [Ge] and Ge/Si ratios makes germanium an effective tracer of hot spring input. We use the Ge/Si mass balance to estimate the spring flux to individual river systems. Our results show that the premonsoon spring flow over the entire Narayani basin is about 2 m^3/s (with a factor of 2 uncertainty), or 0.5% of the total Narayani river discharge. We estimate that the springs provide 25 (±15)% of the silicate-derived alkalinity to the Narayani system during the low-flow season from October to May. Available monsoon season data indicate that the spring flux increases during the monsoon by a factor of 2–3, but this increased flow is diluted by the up to 10× increase in overall river flow. The annual river discharge-weighted mean spring flux is 3.0 ± 1.2 m^3/s for the Narayani; hydrothermal alteration contributes ~10% of the annual flux of silicate alkalinity to this large river system.

Components: 15,037 words, 7 figures, 8 tables.

Keywords: alkalinity; germanium; Himalaya; hot springs; weathering.

Index Terms: 1045 Geochemistry: Low-temperature geochemistry; 1065 Geochemistry: Trace elements (3670); 8135 Tectonophysics: Hydrothermal systems (8424).

Received 20 February 2004; **Revised** 8 June 2004; **Accepted** 8 July 2004; **Published** 25 August 2004.

Evans, M. J., L. A. Derry, and C. France-Lanord (2004), Geothermal fluxes of alkalinity in the Narayani river system of central Nepal, *Geochem. Geophys. Geosyst.*, *5*, Q08011, doi:10.1029/2004GC000719.

1. Introduction

[2] The sources of alkalinity in Himalayan rivers, and the impact of this alkalinity on the world oceans have been of interest to geochemists seeking to evaluate the influence of mountain building on global geochemical cycles [*Sarin et al.*, 1989; *Krishnaswami et al.*, 1992; *Pande et al.*, 1994; *Quade et al.*, 1997; *Dalai et al.*, 2002; *Dowling et al.*, 2003; *Jacobson et al.*, 2003]. In the Ganges-Brahmaputra (GB) river system, independent studies have established that the major source of alkalinity is the dissolution of carbonates, with smaller but variable contribution from silicate alteration [*Galy and France-Lanord*, 1999; *English et al.*, 2000; *Jamieson et al.*, 2002]. These results place limits on the role of silicate weathering in the Himalaya as a long term carbon sink but the processes that generate silicate alkalinity require further quantification. Both climate and geomorphic position appear to play roles in determining silicate weathering fluxes. At the scale of large Himalayan catchments, silicate weathering yields appear to scale with runoff [*France-Lanord et al.*, 2003]. In the high-relief Himalayan zone, silicate weathering in the soil environment is limited by rapid landscape turnover and short residence time of minerals in the soil. Regolith weathering is more extensive in the more stable foreland basin, and silicate weathering yields are substantially higher in the Siwalik zone [*Derry and France-Lanord*, 1997; *West et al.*, 2002; *France-Lanord et al.*, 2003].

[3] Hydrothermal activity along the Himalayan front is another, less well investigated, source of river solutes and alkalinity. Active hot springs are present in all the major river valleys along the topographic front of the central Himalaya. In a previous study we estimated that hot springs are the source of up to 30% of the silicate-derived cations in the Marsyandi river in central Nepal [*Evans et al.*, 2001]. Alteration reactions at hydrothermal temperatures can be an efficient means of neutralizing carbonic acid and generating alkalinity in silicate terranes. The direct introduction of hot spring fluids and the dissolution of hydrothermal precipitates could be significant sources of silicate-derived alkalinity in geothermally active regions, but these fluxes have rarely been quantified in studies of chemical mass balance in river systems. Here we develop a chemical mass balance technique using germanium to estimate the contribution of hot springs to the river discharge, and then compute the contribution of silicate derived alkalinity to the river system of central Nepal from geothermal sources. The results indicate that hydrothermal activity is an important source of silicate derived alkalinity to rivers in this tectonically active region.

2. Geologic Setting

[4] The Himalayan front of central Nepal consists of two north-dipping fault systems that delineate the main lithologic units (Figure 1). Moving from south to north and upsection, the intermediate-grade schists and phyllites of the Lesser Himalayan sequence (LH) are separated from the over-riding high-grade gneisses of the High Himalayan Crystalline units (HHC) by the Main Central Thrust (MCT). Both the LH and HHC are derived from clastic and carbonate sediments deposited off the passive continental margin of India in the Middle to Late Proterozoic, respectively [*Parrish and Hodges*, 1996]. The Main Central Thrust is a 1–10 km wide shear zone [*Le Fort*, 1975]. The South Tibetan Detachment System (STDS) consists of a series of low-angle normal faults [*Burg et al.*, 1984; *Burchfiel and Royden*, 1985; *Hodges et al.*, 1992] dividing the HHC from the overlying Tethyan Sedimentary Sequence (TSS), a Paleozoic to Tertiary low-grade shelf sequence dominated by carbonates. The Narayani river system is composed of four major south-flowing tributaries which flow across all the lithologies of the Himalayan front (Figure 1); these are the Kali Gandaki, the Marsyandi River, the Bhuri Gandaki, and the Bhote Kosi/Trisuli River. Other significant streams sampled in this study include the Mayagdi Khola, the Modi Khola, the Seti Khola, and the Langtang Khola.

3. Hot Springs

[5] Along the base of the High Himalaya, there is a significant topographic break which is generally parallel to and often coincident with the trace of the Main Central Thrust (MCT) [*Seeber and Gornitz*, 1983; *Sai-Halasz*, 1999; *Wobus et al.*, 2003]. Along this topographic break and at or near the MCT, numerous hot springs flow within and along the south-flowing streambeds [*Bhattarai*, 1980]. Typically the springs occur as clusters of individual water sources along a stretch of river bank from tens to over one hundred meters long. A number of spring systems are associated with nick points in stream profiles. Geothermal systems in areas of relatively high regional heat flow often form along

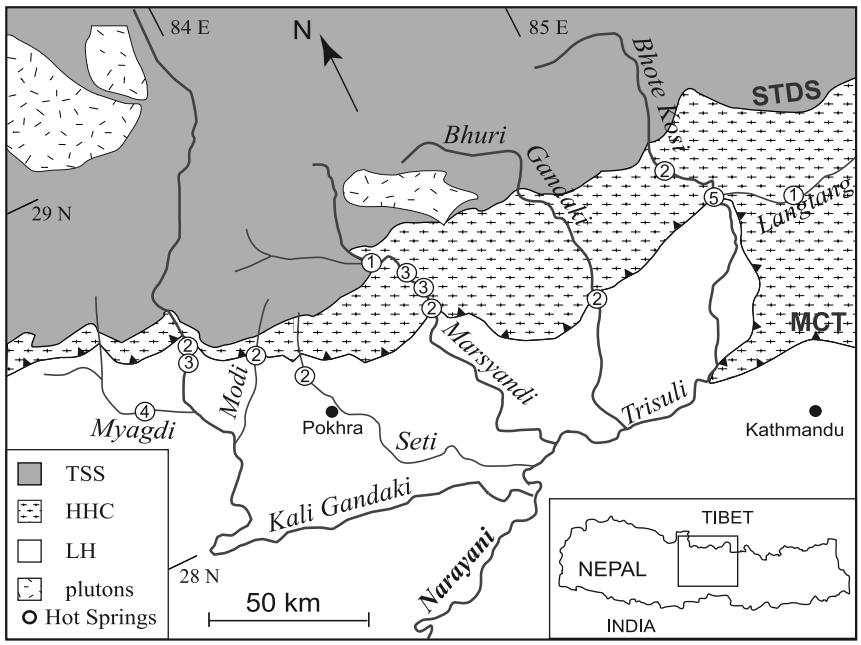

Figure 1. Generalized geologic map [after *Colchen et al.*, 1986] with hot spring locations (open circles). Sampling sites often include several flows from the same spring system. The number within the open circle indicates the number of distinct flows sampled at each location. See Tables 1 and 2 for sample-specific longitude and latitude. Many active hot springs are located near the trace of the Main Central Thrust. Most springs flow from the High Himalayan Crystalline (HHC) or Lesser Himalayan (LH) formations. Springs in the upper Kali Gandaki system flow from the Tethyan Sedimentary Series (TSS) of rocks.

fault/fracture zones and are particularly prevalent where these fracture zones intersect with topographic lows [*Rybach*, 1981]. Similarly, in central Nepal, hot springs tend to flow where the MCT shear zone intersects with the highly incised gorges (Figure 1). The majority of the springs in the study area flow from HHC bedrock although the springs in the Myagdi Khola and a portion of those in the Kali Gandaki and Trisuli flow from Lesser Himalayan rock formations, demonstrating the strong regional topographic control over spring locations. An additional set of springs are found within the N–S trending graben in the upper Kali Gandaki system and flow from TSS lithologies.

4. Methods

[6] River and hot spring samples for this study span multiple field seasons from 1975 to 2001. Water samples were filtered through 0.22 or 0.45 μm filters and stored in acid-washed polyethylene bottles. Two samples were taken from each location; one was acidified with ultra-clean HNO_3 for analysis of dissolved cations. The other was not acidified and taken without head space to minimize degassing, and used for analysis of anions. Every effort was made to minimize exposure to sunlight and ambient temperatures. Samples were refrigerated upon return to Kathmandu, within 1 to 15 days after collection, and after air transport to the laboratory until analysis. Major element concentrations were measured by inductively-coupled-plasma atomic emissions spectrometry (ICP-AES) (cations) and ion chromatography (anions) at Cornell University and the Centre de Recherches Pétrographiques Géochimiques (CRPG), in Nancy, France. Uncertainty on both cation and anion analyses was <5%. Sr isotopic compositions were measured on a VG Sector-54 at Cornell University. Dissolved silica was determined by both ICP-AES and "molybdate blue" spectrophotometry and the results are comparable to within 10%. Ge concentrations were determined by isotope-dilution hydride generation [*Mortlock and Froelich*, 1996] on a Finnigan Element II inductively coupled plasma mass spectrometer (ICP-MS) at Cornell University [*Kurtz*, 2000]. Total reagent blanks for Ge are less than 0.5 ppt and reproducibility is ~3%.

[7] River discharge was measured in the field for the Myagdi Khola, Kali Gandaki, Modi Khola, Seti Khola, and Langtang Khola rivers using a submersible flowmeter (General Oceanics© 2030R) and tape and staff measurements for river width and depth. Discharge measurements were

taken at the same location and at the same time as water samples to reduce potential uncertainty in subsequent calculations. Multiple flow readings were taken at bridge crossings where depth and width could be readily measured. The Nepali Government's Department of Hydrology and Meteorology (DHM) has monitored stream gauges for 10 years and report average monthly discharge for the Bhuri Gandaki, Marsyandi, Trisuli, and Kali Gandaki as well as the Narayani over this 10-year span [*Yogacharya et al.*, 1998]. Uncertainty for these discharge measurements has been estimated at ±25% [*Lave and Avouac*, 2001]. The discharge measured in March, 2001 for this study for the Kali Gandaki at Beni is 58 ± 21 m^3/s (Table 3). The ten year average for March discharge reported by the DHM for the station at Baglung, just downstream from Beni, is 54 ± 13 m^3/s [*Yogacharya et al.*, 1998]. Both values agree well within their reported uncertainties and this provides a level of confidence for the discharge measurement technique used in this study.

5. Results

5.1. River Chemistry

[8] New samples analyzed for this study from central Nepal rivers have temperatures ranging from 8° to 19°C and pH values range from 7.9 to 8.9 (Table 1). As most of the rivers have headwaters in the TSS, carbonate dissolution dominates the cation budget with Ca^{2+} and Mg^{2+} comprising 75 to 95% of the cationic charge, and $Na^+ + K^+$ making up equal portions of the remaining cation budget (Figure 2a). Bicarbonate is the dominant anion (Figure 2b) and the rivers generally have low [Cl^-]. Total dissolved solids (TDS) for the rivers averages around 150 mg/L and is higher in samples downstream of spring locations. The rivers are near or above saturation with respect to calcite. The chemistry of the Trisuli differs somewhat from the other major streams, with a larger contribution to the cationic charge from Na^+ and K^+. *Galy and France-Lanord* [1999] observed that the Bhote Kosi-Trisuli River system is primarily a silicate bedrock drainage basin, and the water chemistry is less affected by carbonate dissolution than are the other major streams.

5.2. Hot Spring Chemistry

[9] The central Nepal hot springs are primarily $Na^+ - HCO_3^- - Ca^{2+} - Cl^-$ waters with circumneutral pH (Table 2). Temperatures of the springs range from 20° to as high as 68°C with an average of 44°C (n = 27). TDS values range from as low as 450 mg/L to 7000 mg/L. The cation balance is dominated by the alkali elements ($Na^+ + K^+$) and Ca^{2+} with minor Mg^{2+} (Figure 2a) while HCO_3^- is typically the principal anion, with concentrations up to 56,000 μmol/kg (Figure 2b). Sulfate levels are generally less than 1000 μmol/kg. Most of the springs are saturated to supersaturated with respect to both calcite and quartz. Several springs in the Marsyandi are Cl^- rich, with up to 114 mmol/kg, while two springs in the Myagdi Khola have very high boron concentrations (up to 2400 μmol/kg). Sr^{2+} concentrations and isotopic compositions are highly variable with [Sr^{2+}] from 167 μmol/kg to <1 μmol/kg and $^{87}Sr/^{86}Sr$ range from typical carbonate values of 0.71 to as enriched as 0.98. The Sr chemistry in the springs appears to be strongly lithology-controlled (Figure 3).

6. Chemical Mass Balance

[10] In order to assess the overall effect of the spring systems across the Narayani drainage the discharge from all the springs must be quantified. Direct measurement of the spring discharge is difficult, as many springs are physically inaccessible and/or are relatively small and diffuse flows which can discharge directly into the streambed. A chemical mass balance approach provides a viable alternative to direct measurement and has the distinct advantage of accounting for springs that are both hard to reach and as of yet un-sampled or unmapped. This approach has long been used in hydrological studies [*Kilpatrick and Cobb*, 1985; *Herschy*, 1995] and was successfully applied to the springs flowing near the MCT in the Marsyandi system [*Evans et al.*, 2001].

6.1. Germanium as a Tracer of Hot Spring Input

[11] Several characteristics must be assessed when choosing an appropriate tracer of hot spring input. Most importantly, the element(s) involved should show conservative behavior during mixing of spring and river waters. In addition, in order for the mass balance to be well resolved there should be a strong contrast between the tracer values in the springs and surface waters. *Evans et al.* [2001] used Cl^- as an effective chemical tracer of hot spring input for the Marsyandi spring system. In this system, the Cl^- concentrations in the springs are up to 4 orders of magnitude higher than those in the tributaries and Cl^- is a conservative element

Table 1 (Representative Sample). Major and Trace Element Data for Central Nepal Rivers[a] [The full Table 1 is available in the HTML version of this article at http://www.g-cubed.org.]

	Latitude, N	Longitude, E	Stream	Date	T, °C	pH	TDS	HCO_3^-	F^-	Cl^-	SO_4^{2-}	B	NO_3^-	Na^+	K^+	Mg^{2+}	Ca^{2+}	Si	Ge/Si
								Myagdi River											
MLB 67	28°22.32′	83°29.77′	Myagdi River	4/3/01	14	8.6	220	2061	5	74	393	2.4	7.7	191	59	470	871	88	5.2
MLB 75	28°20.53′	83°33.79′	Myagdi River	4/3/01	15	8.9	215	2019	6	88	374	6.3	2.3	233	62	446	840	87	13.5
								Kali Gandaki											
MLB 76	28°21.19′	83°33.99′	Kali Gandaki	4/5/01	14	8.8	278	2061	8	473	661	4.3	5.6	656	60	566	1013	87	4.6
MLB 78	28°24.82′	83°36.02′	Kali Gandaki	4/5/01	15	8.8	343	2391	10	645	879	5.1	5.8	902	84	707	1208	97	1.0
MLB 86	28°29.78′	83°39.26′	Kali Gandaki	4/7/01	10	8.5	360	2523	10	734	889	4.6	5.6	852	93	745	1310	101	7.0
NAG 32[b]			Kali Gandaki	12/2/95	2	8.8	416	2811	12	663	1171			833	74	966	1490	92	2.1
NAG 39[b]			Kali Gandaki	12/3/95	9	8.5	361	2624	12	528	906			600	87	771	1371	99	8.2
NAG 43[b]			Kali Gandaki	12/5/95	9		314	2455	8	361	734			423	72	679	1214	92	1.9
NAG 45[b]			Kali Gandaki	12/6/95	13	8.6	231	2004	7	188	433			254	70	451	921	101	4.2
NH 6b			Kali Gandaki	3/12/95	17	8.8	264	2588	8	202	351			269	62	636	948	108	1.4
NH8b			Kali Gandaki	3/13/95	11	8.6	290	2396	9	394	570	3.7		495	54	622	1072	103	7.4
MO 308[c]			Kali Gandaki	7/7/98		8.6	120	1194	4	28	141			61	66	171	520	81	1.4
MO 314[c]			Kali Gandaki	7/8/98		8.7	140	1537	5	23	97			53	48	308	521	118	0.9
MO 500[c]			Kali Gandaki	7/26/98		8.0	180	1514	9	208	832			305	49	505	1015	54	1.5
MO 515[c]			Kali Gandaki	7/27/98			147	1549	9	133	594			212	69	391	908	59	1.4
MO 517[c]			Kali Gandaki	7/27/98		8.6	157	1614	6	153	413			200	72	317	846	60	5.2
LO 1b			Kali Gandaki	5/16/93	14		358	2330	22	770	962	7.3		937	79	761	1244	52	0.7
NAG 5[b]			Kali Gandaki	11/13/93	18	8.4	206	2095	6	93	262			135	49	493	774	59	6.2
								Modi Khola											
MLB 88	28°25.10′	83°49.71′	Modi Khola	4/10/01	9	8.5	145	1336	3	27	266	0.6	7.4	89	40	187	702	67	4.5
MLB 93	28°24.47′	83°49.16′	Kyumunu Khola	4/11/01	10	8.5	188	1639	4	5	439		2.6	76	90	437	744	102	0.4
MLB 94	28°23.65′	83°49.54′	Modi Khola	4/11/01	9	8.6	156	1425	3	22	297	0.5	7.9	103	56	234	714	75	3.2
MLB 98	28°19.30′	83°53.78′	Mardi Khola	4/12/01	19	8.8	138	1498	3	7	138	0.0	2.9	81	53	280	547	124	0.5
								Seti Khola											
MLB 99	28°21.72′	83°57.75′	Seti Khola	4/12/01	12	8.6	214	1894	7	142	402	1.7	9.5	213	54	328	965	85	12.2
MLB 103	28°21.50′	83°57.59′	Seti Khola	4/13/01	12	8.4	204	1697	7	219	415	2.4	8.0	295	57	333	870	91	19.4
MO 200[c]	28°3.00′	84°4.50′	Seti Khola	4/13/01	24	6.0	225	3619		86	257	0.8		168	108	584	1349	100	3.6
MO 304[c]			Seti Khola	7/7/98			129	1424		15	80			46	57	205	543	109	0.9

[a] All concentrations in μmol/kg except TDS in mg/kg and Ge/Si in μmol/mol.
[b] Data previously reported by *Galy and France-Lanord* [1999].
[c] Data previously reported by *France-Lanord et al.* [2003].
[d] Data previously reported by *Evans et al.* [2001].

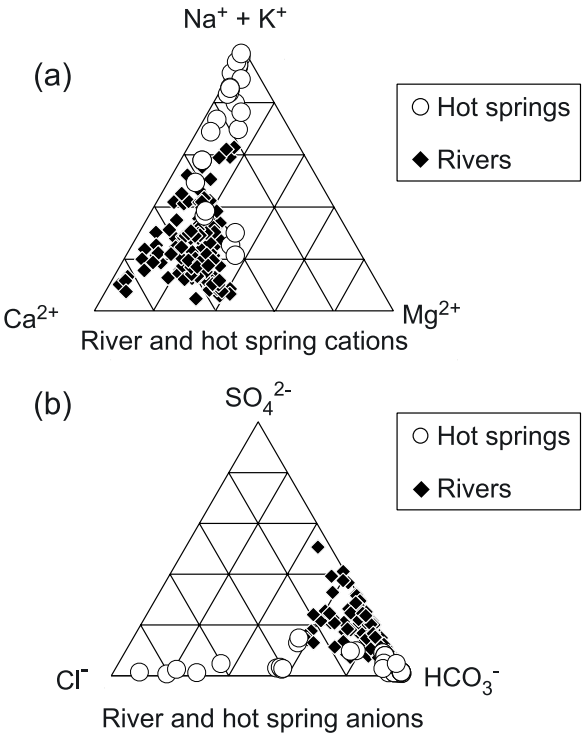

Figure 2. (a) Cation and (b) anion triangular diagrams showing river (filled diamonds) and hot spring (open circles) chemistry. Rivers are dominated by carbonate dissolution, with high Ca^{2+} and Mg^{2+}, while hot springs show a strong silicate alteration influence with Na^{+} and K^{+} making up most of the cation budget. Both river and hot spring anion balances are controlled by bicarbonate with some hot springs showing variable but strong Cl^{-} enrichment.

in this setting. However, the strong Cl^{-} enrichment seen in the Marsyandi springs is not common in the central Nepal spring systems, most of which have relatively low Cl^{-}. Similarly, springs along the Myagdi Khola are highly enriched in boron, but such high B levels are not typical of most other Nepali springs. Germanium levels are ubiquitously high in Himalayan hot springs (Table 2) [*Evans and Derry*, 2002] and the characteristic enrichment of Ge in hydrothermal waters makes it an effective tracer of hot spring input to streams.

6.2. Germanium in Rivers

[12] Germanium and silicon display like behavior in most geological environments due to similarities in both charge and ionic radius. Ge/Si ratios can therefore be used to trace silica behavior during surface processes [*Mortlock and Froelich*, 1987; *Murnane and Stallard*, 1990; *Kurtz et al.*, 2002]. Globally, germanium-silicon systematics in clean rivers (unaffected by coal fly ash pollution) tend to form arrays on Ge/Si versus Si (or 1/Si) plots [*Froelich et al.*, 1985]. This relationship has been interpreted to reflect mixing between weathering of primary minerals which yield high [Si] and low Ge/Si, and weathering of secondary minerals, which yield low [Si] and high Ge/Si [*Mortlock and Froelich*, 1987; *Murnane and Stallard*, 1990; *Kurtz et al.*, 2002]. Rivers with Ge/Si values above 3 μmol/mol are rare and are known only from distinct settings. Areas of high weathering intensity or blackwater streams both in tropical environments can produce streams with Ge/Si values ~2.5 μmol/mol and in some cases, glacial weathering processes can produce low [Si] waters with Ge/Si up to 2 μmol/mol, probably from the breakdown of high Ge/Si biotite [*Chillrud et al.*, 1994; *Anders et al.*, 2003]. Higher values have only been reported from a few locations affected by hydrothermal input and/or possibly sulfide weathering [*Mortlock and Froelich*, 1987; *Anders et al.*, 2003].

[13] The major rivers in central Nepal have anomalously high Ge/Si ratios and do not lie near the global mixing array (Figure 4). A significant number of rivers in the Narayani drainage show Ge/Si values from 3 to 20 μmol/mol and have [Ge] up to 2.6 nmol/kg, (Table 1), the highest reported values for streams not affected by coal-fly ash input (Figure 4). These high Ge/Si values are only found in streams with active hot springs indicating that both the high Ge concentrations and Ge/Si ratios in Himalayan streams result from hot spring input. Further, rivers sampled upstream of the zone of geothermal activity and tributaries without hot springs have lower Ge/Si ratios from 0.2 to 1.6 μmol/mol, (average Ge/Si = 0.7). These values are typical of low to moderate intensity weathering processes in continental rocks and fall near the global Ge/Si mean of 0.5 μmol/mol [*Mortlock and Froelich*, 1987].

6.3. Germanium in Hot Springs

[14] Hydrothermal waters are enriched in Ge regardless of geologic setting (e.g., Iceland [*Arnorsson*, 1984], the Massif Central [*Criaud and Fouillac*, 1986], and the seafloor [*Mortlock et al.*, 1993]). Hot springs in central Nepal have very high germanium concentrations (up to 684 nmol/kg) and some of the highest (Ge/Si) ratios reported for thermal waters with values ranging from 4 to 1000 μmol/mol [*Evans and Derry*, 2002]. The large and consistent contrast between spring and surface waters makes germanium ideal for use in the chemical mass balance (Table 2). Germanium has similar chemical

Table 2 (Representative Sample). Major and Trace Element Data for Central Nepal Hot Springs[a] [The full Table 2 is available in the HTML version of this article at http://www.g-cubed.org.]

	Latitude, N	Longitude, E	Date	T, °C	pH	TDS	HCO_3^-	F^-	Cl^-	SO_4^{2-}	B	NO_3^-	Na^+	K^+	Mg^{2+}	Ca^{2+}	Sr^{2+}	$^{87}Sr/^{86}Sr$	Si	Ge/Si
Myagdi Hot Springs																				
MLB 66	28°22.07′	83°30.15′	4/3/01	51	6.8	1726	12330	267	9368	562	145	78	20513	696	435	1218	8.7		566	675
MLB 68	28°22.11′	83°30.12′	4/3/01	49	6.9	2913	21523	348	15199	761	2383	85	37434	1016	306	914	12.4	0.9267	636	1076
MLB 70	28°22.07′	83°30.15′	4/3/01	51	6.8	1861	13490	283	9711	678	1488	47	22288	747	423	1194	10.0	0.9164	556	696
MLB 71	28°22.07′	83°30.15′	4/3/01	42	7.0	2021	14942	297	10405	606	1571	66	24272	868	399	1222	10.5	0.9167	577	696
NH 30			3/13/95	52	6.5	1474	9805	266	8717	672	1351		16746	1230	465	1280	8.4		570	653
NH 32			3/14/95	54	6.8	2245	14069	218	15825	784			26446	1928	317	1325	11.3	0.9156	642	
Kali Gandaki Hot Springs																				
MLB 81	28°27.47′	83°37.57′	4/6/01	36	8.1	261	1652	291	884	367	63	72	1966	116	133	637	1.3		392	274
MLB 82	28°27.59′	83°37.65′	4/6/01	38	7.9	245	1520	213	784	394	45	93	1663	94	129	688	1.9		468	147
MLB 83	28°28.68′	83°38.45′	4/6/01	43	7.6	249	2238	41	332	270	10	56	946	104	207	894	1.1		569	33
MLB 84	28°28.68′	83°38.45′	4/6/01	54	7.3	218	1881	47	339	229	13	81	1044	104	152	702	1.0		795	42
MLB 85	28°29.78′	83°39.26′	4/7/01	66	6.5	1446	7315	82	12408	879	79	75	12353	1351	1339	2243	14.2		815	93
MO 520			7/27/98				15949	63	9669				8012	1397	1108	2181	12.5	0.7963	653	85
DG9936			3/15/99		7.2				2651		9		2446	165	1375	3308	19.2		159	11
DG9937			3/15/99		7.2				6982		45		6407	1090	876	2320	9.1		712	70
NAG 17			11/21/95	30	8	1094	16846	137	347	781	22		17181	827	131	309	1.1	0.7336	207	
NH 9			3/14/95	69	6.5	1286	6470	78	10635	889			11375	1696	1263	1669	12.8		835	
NH 11			3/15/95	50	6.7	1670	8814	63	14979	422	74		15268	1512	774	3214	9.9	0.8103	623	79
NH 12			3/15/95	60	7.4	225	2008	58	316	265	9		1227	176	70	689	1.4		850	43
LO 46			5/20/93			511	5645	36	136	332			655	101	348	2509	6.4			
LO 47			5/20/93	20		8587	36424	316	93089	131	365		111048	7581	3662	2085	167.2	0.7306	339	
LO 65			5/21/93	13		1692	19971	137	1206	42	28		8356	1172	3436	2473	39.8	0.7169	1220	
LO 105			5/27/93	21		953	5718	55	2807	2598	9		2705	171	2218	3216	21.3			
Modi Khola Hot Springs																				
MLB 87	28°24.94′	83°49.71′	4/10/01	39	6.8	734	7714	13	248	751	2	90	1752	166	1007	2392	4.4		532	21
MLB 92	28°24.94′	83°49.71′	4/10/01	39	7.0	809	8716	15	265	723	2	86	2007	201	1072	2534	4.7		501	20
DG9939			3/15/99						312				125	127	1059	2068	5.2		524	16
Seti Khola Hot Springs																				
MLB 101	28°21.65′	83°57.61′	4/13/01	45	6.5	4630	54865	7	248	216	102	4	41096	1876	1449	4821	18.0	0.8203	1102	268
MLB 102	28°21.65′	83°57.61′	4/13/01	43	6.3	3530	41620	6	575	165	85	5	29674	1489	1253	4431	16.7	0.7981	830	265
NH 37			3/16/95	43	6.2	2925	16134	90	19379	3248	74		28230	1547	1189	4998	11.9		827	199
NH 38			3/16/95	41	6.5	3403	15381	111	26573	3956	93		38495	2261	1300	3346	10.2	0.8162	967	

[a] All concentrations in μmol/kg except TDS in mg/kg and Ge/Si in μmol/mol. Note: Series DG-99 data are incomplete with $[HCO_3^-]$ not calculated for some samples due to a lack of SO_4^{2-} analyses. The remaining data are reported for completeness.

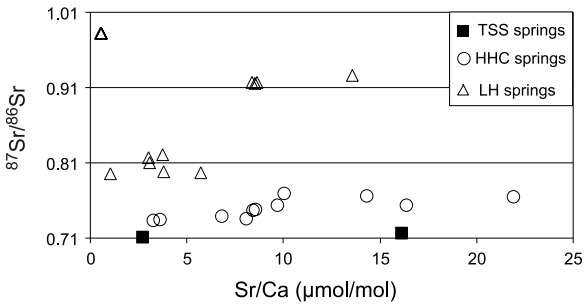

Figure 3. Sr/Ca (μmol/mol) versus $^{87}Sr/^{86}Sr$ in the hot springs. The Sr chemistry of the springs reflects that of the bedrock at the spring outlet. Springs flowing from the Tethyan Sedimentary Series (TSS) have typical carbonate $^{87}Sr/^{86}Sr$ (0.712–0.717) and variable Sr/Ca. Lesser Himalayan (LH) springs have lower Sr/Ca values and very radiogenic $^{87}Sr/^{86}Sr$ up to 0.98. Springs that flow from High Himalayan Crystalline (HHC) rocks have higher Sr/Ca and $^{87}Sr/^{86}Sr$ that ranges from 0.73 to 0.77. Each of these ranges in $^{87}Sr/^{86}Sr$ is consistent with bedrock values found in the host formations [*France-Lanord et al.*, 1993]. The strong reflection of the local lithology in the spring waters indicates an areally limited flow path for hydrothermal waters.

behavior to silicon and would only be removed from streams in significant amounts by opal precipitation. Himalayan streams are strongly undersaturated with respect to opal and Ge should therefore be conservative. In some environments sorption of Ge to iron oxides may affect Ge/Si systematics [*Anders et al.*, 2003]. Some of the hot springs, particularly those known locally as "ratopani" ("colored water") precipitate iron oxides around the spring vent. Ge/Si ratios in two oxide precipitates were 0.14 and 3.8 (Table 2). On the basis of this limited data set, we make the assumption that Ge is not significantly fractionated from silica in this environment. While strong enrichment in Ge is ubiquitous in the hot springs in our study area, the degree of enrichment is quite variable between individual spring systems. Consequently, we calculate the influence of hydrothermal discharge on river chemistry using measured values from individual river and spring systems.

6.4. Hot Spring Discharge

[15] The fraction of the total river discharge contributed by the hot springs (F_W^{HS}) is calculated using an end-member mixing model for Ge/Si ratios, weighted by the silica concentration of the end-members (equation (1)). End-members are the tributaries or upstream reaches of the rivers unaffected by hot spring input, and the hot springs. We make the assumptions that the Ge/Si in the main stem is the weighted sum of the hot spring and tributary contributions and that Ge and Si behave conservatively during mixing:

$$F_W^{HS} = \frac{Q_{HS}}{Q_{trib}} = \frac{[Si]_{trib}}{[Si]_{HS}} \times \frac{\left(\frac{Ge}{Si}\right)_R - \left(\frac{Ge}{Si}\right)_{trib}}{\left(\frac{Ge}{Si}\right)_{HS} - \left(\frac{Ge}{Si}\right)_R}, \qquad (1)$$

F_W^{HS} is the fraction of the total river discharge contributed by the hot springs. Square brackets denote concentrations. Subscript *HS* denotes average hot spring values for each basin, *trib* denotes all nonspring affected surface water input (including the main stem upstream of the hot springs, surface runoff, and cold springs), and *R* denotes downstream value for the main stem taken near the point of measurement for the main stem discharge.

[16] F_W^{HS} was determined for the spring systems in each of the eight major individual drainages (Myagdi, Kali, Modi, Seti, Marsyandi, Bhuri, Trisuli/BhoteKosi, and Langtang) that contribute to the Narayani system. Tributaries and upstream values from locations without known springs and showing no chemical effect of spring input (low Ge/Si, low $[Cl^-]$) were averaged to produce a consistent surface water input for all the drainages. The resulting values are $(Ge/Si)_{trib} = 0.7 \pm 0.46$ μmol/mol and $[Si]_{trib} = 155 \pm 38$ μmol/kg (n = 21, uncertainties given as 1 standard deviation). $(Ge/Si)_{HS}$ and $[Si]_{HS}$ are average values for the sampled springs in each drainage. Calculated F_W^{HS} ranges from as little as 0.1% of the total river flow for the Langtang Khola to as high as 4.2% for the Modi Khola (Table 3). Actual discharge from the hot springs was calculated using main stem discharge values from two sources. When possible, river discharge was measured in the field to reduce potential temporal and geographic uncertainties. Where field-discharge measurements were not available, the DHM 10-year average for the sampling-month was used [*Yogacharya et al.*, 1998]. It is important to note that the spring discharge values calculated here are based on dry-season sampling, the Myagdi, Kali, Modi, Seti, Marsyandi, Trisuli, and Langtang in March/April of 2001 and the Bhuri in October 1999. The F_W^{HS} is therefore the fraction of total flow derived from the springs during the low-flow times of the year. For the sum of the 8 watersheds, $F_W^{HS} = 0.52 \pm 0.3\%$, equivalent to a

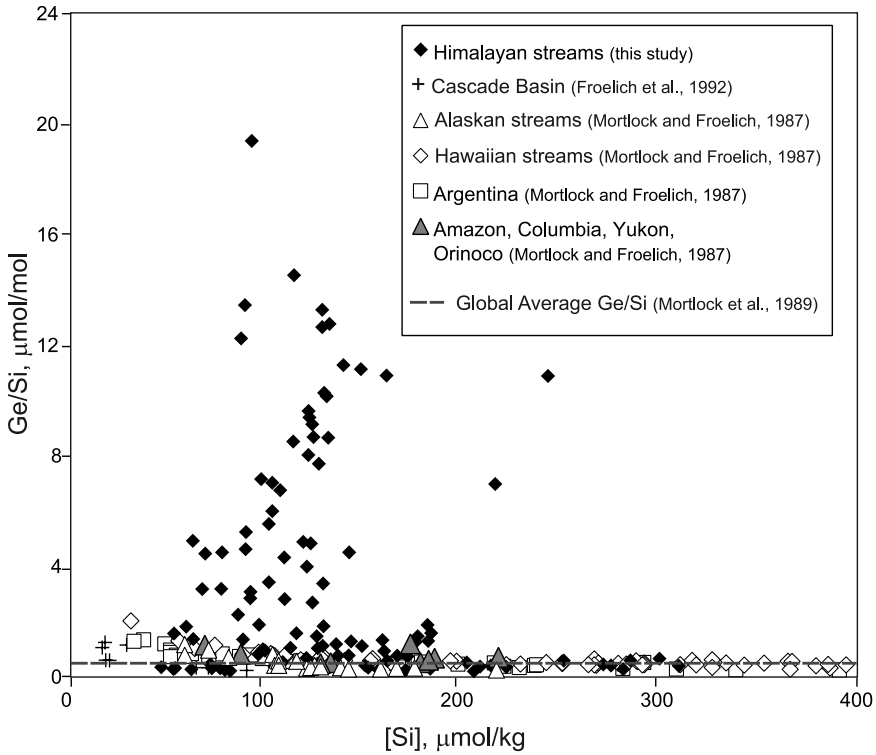

Figure 4. Ge/Si versus [Si] for reported world rivers (open symbols) [*Froelich et al.*, 1985, 1992; *Mortlock and Froelich*, 1987; *Chillrud et al.*, 1994]. Himalayan river Ge/Si values (filled diamonds) range from near the world average of 0.5 μmol/mol (gray dashed line) to as high as 20 μmol/mol, the highest values reported for nonpolluted streams. Smaller Himalayan streams with no known hydrothermal inputs have Ge/Si near the world average, while those with Ge/Si between 2 and 20 μmol/mol are sampled near or downstream of hot spring locations.

discharge of ≈2 m^3/s across the entire Narayani basin.

6.5. Uncertainties

[17] Overall uncertainties for F_W^{HS} are dominated by the uncertainty that arises in determining the hot spring end-member Ge/Si value. While the relative uncertainties are large (∼60%) for the tributary end-member Ge/Si value, this has a relatively minor effect on the F_W^{HS} calculation. In systems with only one sampled spring the end-members are easily defined and the uncertainty is relatively small (i.e., the Modi Khola). However, in the Marsyandi, Kali Gandaki and Trisuli river systems there are multiple spring locations (Figure 1) with variable Ge systematics and this variability results in increased uncertainty when defining a hot spring end-member value for the mass balance. The uncertainty on F_W^{HS} is compounded following typical error propagation protocol [*Ku*, 1969].

6.6. Comparison With Cl^- Mass Balance

[18] The Marsyandi river system has been well sampled, and the hot springs are found in four clusters within the outcrop area of the HHC above the Main Central Thrust [*Evans et al.*, 2001]. Downstream profiles of chloride (and other elements) and Ge/Si ratios clearly show the impact of hot spring input (Figure 5). In the headwaters, both the main stem and tributaries have Ge/Si = 0.3 μmol/mol. A zone of hot springs 30 km from the headwaters near Chame have Ge/Si from 60–110 μmol/mol, and the main stem value increases as it passes through this zone. Near Jagat, (55 km from the headwaters) a second group of hot springs with Ge/Si near 180 μmol/mol drive the main stem ratio to over 10, while tributary values remain <1.8 μmol/mol. Near Bahundada (∼65 km from the headwaters and a few km upstream of the surface expression of the MCT), springs with Ge/Si ≈ 50 and two tributaries with Ge/Si ≈ 11 maintain a high ratio in the main stem, despite the contribution of other "normal" tributaries with low Ge/Si. The two anomalous tributaries near Bahundada almost certainly have hot spring input, although we did not explore them upstream. One (Ngadi Khola) has high chloride, consistent with geothermal activity. Downstream, dilution by tributaries with typical weathering values of

Table 3. Fraction of the Total River Discharge Contributed by the Hot Springs (F_W^{HS}) for the Rivers of the Narayani Basin[a]

	River Sample	Q_R, m^3/s	$[Si]_R$, μmol/kg	$(Ge/Si)_R$, μmol/mol	$[Si]_{HS}$, μmol/kg	$(Ge/Si)_{HS}$, μmol/mol	Hot Spring Sample(s)	F_W^{HS}, %	Q_{HS}, m^3/s
Myagdi	MLB 75	52[b]	86	13.5	584	795	MLB 66, 68, 70, 71	0.4	0.23 ± 0.09
Kali	MLB 76	58[b]	87	5.4	607	100	MLB 81, 82, 83, 84, 85	1.3	0.74 ± 0.67
Modi	MLB 94	7[b]	74	3.2	517	21	MLB 87, 92	4.2	0.29 ± 0.11
Seti	MO 200	28[c]	99	3.6	966	267	MLB 101, 102	0.2	0.05 ± 0.02
Marsyandi	MO 2	40[d]	100	6.0	1306	131	MLB 51, 55, 58	0.5	0.20 ± 0.14
Bhuri	GA 240	169[d]	93	1.9	977	129	GA 217	0.2	0.25 ± 0.14
Trisuli	Tri-4-4-94	40[d]	124	8.6	2053	80	MLB 27, 28, 4, 5	0.8	0.33 ± 0.30
Langtang	MLB 32	5[b]	125	3.4	832	583	MLB 41	0.1	0.004 ± 0.001
Sum		399							2.1 ± 2.0

[a] The fraction of the total river discharge contributed by the hot springs is F_W^{HS}. Values are calculated from equation (1) for the dry season using $[Si]_{trib}$ = 155 μmol/kg and $(Ge/Si)_{trib}$ = 0.7 μmol/mol.
[b] Discharge measured in field.
[c] Discharge from *Hurtrez* [1998].
[d] Discharge from *Yogacharya et al.* [1998].

Ge/Si ≤ 1 causes the main stem Ge/Si ratio to fall to 4.5 μmol/mol just before its confluence with the Trisuli. The overall pattern of Ge/Si in the Marsyandi is very similar to that for chloride. We can compare the result of the Ge/Si mass balance calculation with that based on Cl^-. Average $[Cl^-]$ of the Marsyandi tributaries is 34 μM and that of the hot springs 57,000 μM. With a simple mass balance, a fractional spring discharge of 0.52 ± 0.4% yields the observed $[Cl^-]$ of 366 μM at the Marsyandi-Trisuli confluence. The Ge/Si mass balance for the Marsyandi yields a F_W^{HS} of 0.50 ± 0.35% and agrees well with the Cl mass balance of *Evans et al.* [2001]. The close agreement of these two independent tracers of hydrothermal input strongly suggests that the Ge/Si mass balance is a viable tool for estimating hot spring fluxes.

7. Alkalinity Flux

[19] In light of efforts to quantify the silicate and carbonate weathering fluxes and therefore estimate the effect of weathering in the Himalaya on atmospheric CO_2 budgets, the silicate alkalinity flux from Himalayan rivers has been the focus of recent study [*Sarin et al.*, 1989, 1992; *Singh et al.*, 1998; *Galy and France-Lanord*, 1999; *English et al.*, 2000]. The solute load of the Ganges-Brahmaputra system has been shown to be dominated by carbonate dissolution [*Sarin et al.*, 1989; *Galy and France-Lanord*, 1999; *Jacobson and Blum*, 2000] with an estimated 80–90% of the cations derived from carbonate sources. Nonetheless, for drainages underlain with silicate bedrock the fraction of total alkalinity derived from silicate sources can exceed 70% [*Galy and France-Lanord*, 1999]. In those silicate-dominated catchments atmospheric deposition and dissolution of trace/minor amounts of carbonate supply the remainder of the riverine alkalinity [e.g., *Jacobson and Blum*, 2000].

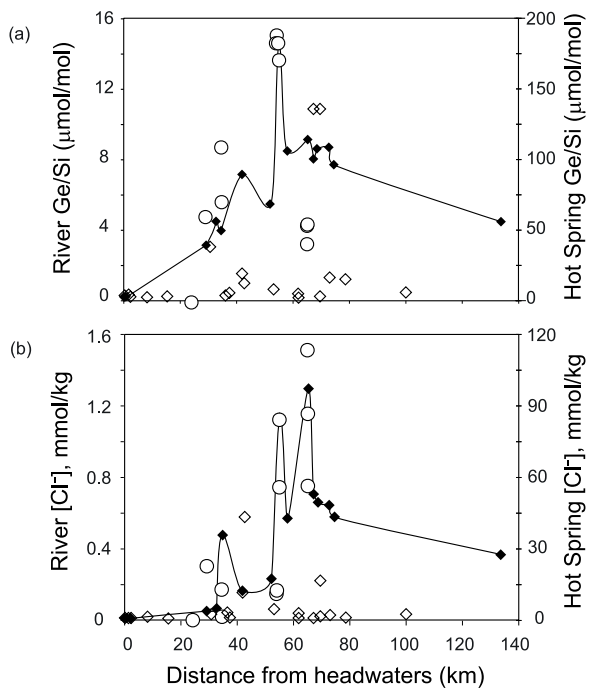

Figure 5. Downstream profile of (a) Ge/Si and (b) $[Cl^-]$ for the tributaries (open diamonds), hot springs (open circles), and main stem (filled diamonds) of the Marsyandi River basin. Note the different scale for hot spring samples on the right-hand y axis. Tributary values are too low to have produced the anomalously high main stem values. The largest spikes in river water $[Cl^-]$ and Ge/Si are just downstream from major hot spring sources. The influence of the hydrothermal input on stream chemistry persists 60 km downstream to the confluence with the Trisuli.

[20] In the Nepal hydrothermal waters, bicarbonate is the dominant anion in all but a few of the springs, and Na^+ and K^+ make up a significant fraction of the total cations (Figure 2). Most of the springs have circum-neutral pH values and relatively low B concentrations; we therefore assume that alkalinity $\cong [HCO_3^-]$. In the Myagdi Khola hot springs, where B concentrations are very high (up to 2400 μmol/kg), this assumption is still valid, as the pH of the springs is ~7 and most of the B should be present as the charge-neutral species $B(OH)_3$ [*Hemming and Hanson*, 1992]. Alkalinity titrations were performed on SPA-97 samples (Tables 1 and 2) and agree to within 10% with the alkalinity estimated via charge balance.

[21] Silicate alkalinity ($[ALK]_{sil}$) is the component of the total alkalinity balanced by cations released by the alteration of silicate minerals. In most natural waters, the alkalinity budget is dominated by Ca^{2+} (and to a lesser extent Mg^{2+}) released by carbonate dissolution. Ordinarily, Na^+ and K^+ do not have significant carbonate sources, and are derived either from silicates, evaporites, or cyclic salts delivered from the ocean inland via precipitation. In stream waters, sodium budgets are often corrected for cyclic salt inputs by attributing all chloride to a "halite" source, with the remainder of Na^+ assigned to silicate sources [*Stallard and Edmond*, 1981]. Given that the Himalayan hot springs we sampled are mostly found within high-grade silicate terranes, we would expect that most of the base cations (Na^+, K^+, Ca^{2+} and Mg^{2+}) are likely to be derived ultimately from silicate mineral alteration. In most spring samples, Cl^- is a minor component of the anionic charge balance, and thus any "cyclic salt" correction is small. The generally low Cl^- levels are consistent with the lack of evidence to suggest a proximal source of halite anywhere in the field area (either sedimentary evaporitic facies, or metamorphic parageneses such as scapolite formation). However, a number of hot spring samples have a larger contribution from Cl^-, and several samples have molar $Na^+/Cl^- < 1$. Stoichiometry indicates that all the Cl^- in these fluids cannot be attributed to halite, and requires that there is another source of Cl^- for the hot springs. The high Cl^- springs are from the Marsyandi basin and are found within the silicate Formation I (FI) of the HHC. We cannot identify the source of high chloride with certainty, but suggest that a plausible source is HCl from metamorphic fluids, possibly derived from a Cl_2 vapor phase produced during metamorphism of subducted LH sediments. Acid generated by the dissociation of HCl would be neutralized by mineral dissolution releasing base cations to solution, and this process could account for the low Na^+/Cl^- ratios.

[22] It remains likely that cyclic salts/halite supply some Na^+ and Cl^- to hot spring fluids. Thus we can estimate the contribution of silicate sources to the alkalinity budget in two ways. A minimum value for silicate alkalinity can be calculated from sodium (corrected for cyclic salts and evaporite dissolution) and potassium:

$$[ALK]_{sil} = [Na^{**}] + [K^+]. \quad (2)$$

[23] However, for the subset with excess Cl^-, equation (2) cannot yield viable estimates because $[Na^{**}] < 0$. Furthermore, this calculation implicitly assumes that all Ca^{2+} and Mg^{2+} are derived from carbonate dissolution, an unrealistic assumption for dominantly silicate lithologies such as FI of the HHC. For the springs with $Na^+/Cl^- < 1$, we conservatively estimated that 30% of the Cl^- is from a nonhalite source, equivalent to assigning all the Na^+ in the most chloride rich spring (MLB-51) to halite (Table 4a) (i.e., no sodium released by silicate alteration), which as we noted above is highly unlikely. For all other springs we assumed 100% of chloride from halite, again almost certainly an overly conservative assumption. However, since chloride is not a major contributor to the charge balance of most of the other springs, the effect of any "cyclic salt" correction on them is small.

[24] The contribution of Ca^{2+} and Mg^{2+} from silicate sources can be estimated using the Ca/Na and Mg/K ratios of host rocks following *Galy and France-Lanord* [1999], who modeled the contribution of silicate-derived Ca^{2+} and Mg^{2+} to the stream alkalinity budget using an equation of the form

$$F_{sil}^{HS} = \frac{[\alpha \times Na^*] + [\beta \times K^+]}{[ALK]_T^{HS}}, \quad (3)$$

where α and β were estimated from HHC feldspars and stream chemistry of silicate only catchments, respectively, $[ALK]_T^{HS}$ is the total alkalinity concentration in the hot spring fluid, and F_{sil}^{HS} is the fraction of the total hot spring alkalinity derived from silicate sources. Feldspars in the HHC are typically An_{18-30}, while whole rock Ca/Na ≈ 0.25 mol/mol [*Galy and France-Lanord*, 1999]. Biotite is a significant reservoir for Mg, with HHC whole rock Mg/K ≈ 0.67 mol/mol [*France-Lanord*

Table 4a. F_{sil}^{HS} Values for Central Nepal Hot Springs From Equation (3)[a]

Drainage	$[ALK]_T^{HS}$, μmol/kg	Na**, μmol/kg	Na** − 0.3Cl⁻, μmol/kg	K*, μmol/kg	1.25Na** + 1.67K*, μmol/kg	F_{sil}^{HS}, %
			Myagdi River			
MLB 66	12330	11143		696	15091	100
MLB 68	21523	22232		1016	29487	100
MLB 70	13490	12574		747	16965	100
MLB 71	14942	13864		868	18779	100
			Kali Gandaki			
MLB 81	1652	1080		116	1543	93
MLB 82	1520	876		94	1252	82
MLB 83	2238	611		104	937	42
MLB 84	1881	702		104	1051	56
MLB 85	7315	−57	3760	1351	6956	95
			Modi Khola			
MLB 87	7714	1501		166	2153	28
MLB 92	8716	1740		201	2510	29
			Seti Khola			
MLB 101	54865	40846		1876	54192	99
MLB 102	41620	29097		1489	38858	93
			Marsyandi			
MLB 51	12223	−35137	0	13031	21761	100
MLB 55	20318	−2793	23380	6072	39365	100
MLB 58	3418	2699		70	3489	100
			Bhuri Gandaki			
GA 217	19146	14034		1168	19493	100
			Bhote Kosi/Trisuli			
MLB 4	10739	7395		634	10303	96
MLB 5	10305	7056		624	9862	96
MLB 27	19166	8873		1948	14344	75
MLB 28	20697	10588		2363	17181	83
MLB 20	7152	791		234	1380	19
MLB 21	6563	654		118	1015	15
MLB 23	6952	913		311	1661	24
			Langtang			
MLB 41	5060	5708		153	7390	100

[a] All concentrations in μmol/kg. Note for those samples where Na** < 0, we have conservatively assigned 30% of the Cl^- to a nonhalite source, equivalent to assigning all the Na^+ in the most chloride rich spring (MLB-51) to halite.

and Derry, 1997]. It is reasonable to suppose that Ca is released by alteration at least as efficiently as Na, as both are dominantly hosted in plagioclase. The relative behavior of Mg and K during alteration is less clear, but because Na*/K is nearly always >4, any uncertainty on the correct Mg/K ratio used to estimate the silicate contribution of Mg will have a small impact on the overall budget uncertainty. On the basis of the above observations, we adopt values of $\alpha = 1.25$ and $\beta = 1.67$, somewhat more conservative than those estimated by *Galy and France-Lanord* [1999], who used $\alpha = 1.4$ and $\beta = 2$, although the difference in F_{sil}^{HS} values obtained using our values or those used by *Galy and France-Lanord* [1999] is small. Assuming zero Ca and Mg derived from silicate alteration (e.g., equation (2)) is equivalent to setting $\alpha = \beta = 1$ in equation (3).

[25] Values of F_{sil}^{HS} were calculated using $\alpha = \beta = 1$ (no Ca and Mg from silicates), and using $\alpha = 1.25$ and $\beta = 1.67$ to estimate the contribution of Ca and Mg from silicates to the alkalinity budget for each spring. The results are broadly similar, because Na and K dominate the alkalinity budget of most of the springs, alone accounting for ≥50% of the alkalinity in 19 of 26 samples. With the estimated contribution from Ca and Mg included, F_{sil}^{HS} is 80–100% for most springs (Table 4a). Two sets of springs, the low-temperature (~20°C) springs in

Table 4b. Seasonal and Annual F^R_{sil} Values for the Major Rivers in the Narayani From Equation (3)

	River	$[ALK]^R_{sil}$, μmol/kg	Na**, μmol/kg	K*, μmol/kg	1.25Na** + 1.67K*, μmol/kg	F^R_{sil}, %
			Seasonal			
MLB 75	Myagdi	1971	134	60	269	14
MLB 76	Kali	2014	173	58	312	16
MLB 88	Modi	1288	51	38	128	10
MO 200	Seti	3572	72	105	267	7
MO 2	Marsyandi	2032	30	58	134	7
GA 240	Bhuri	1430	101	21	162	11
TRI4-4-94	Trisuli	1020	141	41	245	24
MLB 32	Langtang	384	103	5	137	36
NH 1, MO 215[a]	Narayani	2256	90	59	211	9
			Annual			
[b]	Myagdi	1254	83	55	195	16
[c]	Kali	1413	4264	160	11	
[b]	Modi	820	31	35	97	12
[c]	Seti	1962	43	68	166	8
[c]	Marsyandi	1224	38	57	143	12
[b]	Bhuri	910	62	19	110	12
[c]	Trisuli	706	53	37	129	18
[b]	Langtang	244	63	5	87	35
[c]	Narayani	1556	55	58	166	11

[a] Narayani seasonal values calculated from the average of samples NH 1 and MO 215.
[b] Alkalinity values calculated from dilution factors derived from samples with available AWM data (footnote c).
[c] AWM values taken from *France-Lanord et al.* [2003].

the Bhote Kosi (MLB 20, 21, 23), which are found in LH outcrop, and the upper Kali Gandaki springs (MLB 83, 85, 87) have F^{HS}_{sil} values between 20% and 30%, implying a higher percentage of carbonate dissolution locally. For all others, F^{HS}_{sil} is at or close to 100%, indicating that alteration of silicates rather than carbonates is the dominant process producing alkalinity in the hot springs. The actual production of alkalinity by hydrothermal alteration of silicates must be substantially higher than we observe in solution at the spring vent as carbonate precipitation both at the surface and in the subsurface removes significant quantities of alkalinity from solution in all the hydrothermal systems we sampled. This last observation is an important one for understanding the overall role that hydrothermal systems have in setting the alkalinity budget of Himalayan rivers, and we will return to it below.

7.1. Contribution of Hot Springs to River Alkalinity Budgets

[26] The silicate alkalinity fraction F^R_{sil} in the rivers is computed similarly to the hot springs, using equation (3) with $\alpha = 1.25$ and $\beta = 1.67$ and $[ALK]^R_{sil}$ in the denominator. The data used for the river calculations are corrected for atmospheric deposition of solutes using precipitation data from *Galy and France-Lanord* [1999]. F^R_{sil} values for the rivers of the Narayani basin vary from 7% to 36%, with higher values in those rivers dominantly underlain by silicate rocks (Table 4b). We combine the computed fractional hydrothermal water flux F^{HS}_W (equation (1)) with river discharge Q_T and the alkalinity fraction estimates to compute the component of the river flux of silicate alkalinity that is derived from hot springs. The flux of silicate alkalinity in the river, $J\,(ALK^R_{sil})$ is given by

$$J\left(ALK^R_{sil}\right) = Q_T\left(F^R_{sil}\cdot[ALK]^R_T\right), \tag{4}$$

where $[ALK]^R_T$ is the total riverine alkalinity concentration and the total river water discharge $Q_T = Q_{trib} + Q_{HS}$ where Q_{trib} = the discharge of all nonhydrothermal waters. Because Q_{HS} is small relative to Q_{trib}, $Q_T \approx Q_{trib}$. Similarly, the hot spring silicate alkalinity flux $J\,(ALK^{HS}_{sil})$ is given by

$$J\left(ALK^{HS}_{sil}\right) = F^{HS}_W\cdot Q_T\left(F^{HS}_{sil}\cdot[ALK]^{HS}_T\right). \tag{5}$$

Combining equations (4) and (5) yields the fractional contribution of hot springs to the riverine

Table 5. Dry-Season $X\,(ALK_{sil}^{HS})$ Values From Equation (6) for Streams of the Narayani Basin

	Stream Samples	Q_R, m^3/s	1.25Na** + 1.67K* Rivers	$J(ALK_{sil}^{R})$, mol/s	Q_{HS}, m^3/s	1.25Na** + 1.67K* Hot Springs	$J(ALK_{sil}^{HS})$, mol/s	$X(ALK_{sil}^{HS})$, %	Hot Spring Samples
Myagdi	MLB 75	52	269	14.0	0.23	15571	3.52	25 ± 16	MLB 66, 68, 70, 71
Kali	MLB 76	58	312	18.1	0.74	2348	1.74	10 ± 13	MLB 81, 82, 83, 84, 85
Modi	MLB 88	7	128	0.9	0.29	2332	0.68	77 ± 34	MLB 87, 92
Seti	MO 200	28	267	7.5	0.05	46525	2.30	31 ± 17	MLB 101 102
Marsyandi	MO 2	40	134	5.4	0.20	11986	2.41	45 ± 44	MLB 51, 55, 58
Bhuri	GA 240	169	162	27.3	0.25	19146	4.82	18 ± 11	GA 217
Trisuli	TRI4-4-94	40	245	9.8	0.33	12923	4.30	44 ± 43	MLB 27, 28, 4, 5
Langtang	MLB 32	5	137	0.7	0.004	5060	0.02	3 ± 2	MLB 41
SUM		399		83.6	2.1	1.2×10^5	19.8	**24**	
Narayani	NH 1, MO 215	368[a]	211.1	77.7				**25**	

[a] Q_R for the Narayani from *Yogacharya et al.* [1998].

alkalinity flux $X(ALK_{sil}^{HS})$ and eliminates the discharge terms and their uncertainties:

$$X\left(ALK_{sil}^{HS}\right) = \frac{J\left(ALK_{sil}^{HS}\right)}{J\left(ALK_{sil}^{R}\right)} = \frac{F_W^{HS} \cdot F_{sil}^{HS} \cdot [ALK]_T^{HS}}{F_{sil}^{R} \cdot [ALK]_T^{R}}. \quad (6)$$

[27] We find that the hot springs provide from 3 to 77% of the silicate alkalinity to individual rivers (Table 5). The highest and lowest computed values are from the Modi and Langtang basins respectively, which have substantially smaller discharges than the other rivers in our study and contribute least to the overall mass balance. The larger rivers (n = 6) yield $X(ALK_{sil}^{HS})$ = 9 to 27%. Taking the Narayani system as a whole, the hot springs are the source of nearly a quarter of the total silicate alkalinity. The Trisuli, Bhuri, Myagdi and Seti account for nearly 80% of this hydrothermal contribution.

[28] The above alkalinity mass balance of the Narayani system is estimated from the discharge-weighted sum of the silicate alkalinity contributions from the eight major tributaries (Table 5). We also calculate the fraction of hot spring alkalinity relative to the data-driven $J(ALK_{sil}^{R})$ at Narayanigat, downstream of the major confluences. The agreement between the two estimates is encouraging, but it should be noted that the hydrothermal flux value $J(ALK_{sil}^{HS})$ is not independently computed for the second calculation. The agreement results from the fact that the weighted sum of the F_{sil}^{R} from the major tributaries is close to that calculated independently on the basis of the chemistry of the Narayanigat samples, and provides some confidence in the summation procedure. The mass balances presented in Table 5 are constructed primarily from samples taken in the March–May period, which is the low-water season in Nepal. Under these conditions, our results show that geothermal activity is an important source of silicate-derived alkalinity to this major river system, supplying up to one quarter of the total alkalinity derived from silicate alteration in the basin. A substantial flux of carbonic acid is neutralized during hydrothermal reactions to produce the observed hot spring alkalinity. Once the products (cations, bicarbonate) of these reactions are introduced into stream water, they behave as any other alteration (i.e., "weathering") products. We have previously termed this process "high-temperature weathering", as it produces a solute signature largely indistinguishable from "normal" weathering reactions that take place at ambient temperatures within soil and groundwater environments [*Evans et al.*, 2001]. That the small hydrothermal water flux (<1% of the stream discharge) accounts for such a large fraction (>25%) of the silicate alteration budget is a function of the much more efficient reaction kinetics in high-temperature hydrothermal reactions as compared to soil reactions.

7.2. Strontium

[29] Strontium/calcium ratios and $^{87}Sr/^{86}Sr$ values in the hot spring fluids are consistent with derivation of solutes from local host rocks, modified by calcite precipitation [*Evans et al.*, 2001]. Springs found in TSS outcrop have low $^{87}Sr/^{86}Sr$, 0.712–0.717 (Table 2, Figure 3). Values for HHC-sourced springs are more radiogenic and within the range expected for HHC rocks (0.734–0.768) and springs located in LH outcrop are highly radiogenic (0.79–0.98). Springs in LH rocks on average have lower Sr/Ca than the HCC springs,

again consistent with the differences in bedrock chemistry [*Galy and France-Lanord*, 1999]. However, Sr/Ca ratios in the springs are fractionated by the precipitation of calcite [*Evans et al.*, 2001], and the variable extent of calcite precipitation combines with source rock variations to produce a wide spread in Sr/Ca, regardless of source rock (Figure 3). In most cases, the hot spring fluids contribute radiogenic Sr with high Sr/Ca to Himalayan rivers (Table 2). On the basis of the calculated hot spring discharge and the [Sr] of the hot springs and assuming a closed system, the estimate hot spring Sr flux to rivers is variable, ranging from less than a percent in the Langtang to as high as 20% for the Modi and Marsyandi rivers. For the Narayani as a whole, the springs contribute ~6% of the total Sr. For the springs flowing from HHC and LH rock in particular, the radiogenic Sr flux from the springs is significant.

8. Seasonal Variability and Annual Flux Estimates

[30] The monsoon climate of the Himalayan region imposes large seasonal variations in river fluxes of water, solutes and sediments. The majority of geochemical data published for Himalayan rivers are from outside the monsoon period (June–September), including much of the data in this study. However there are sufficient data to make a preliminary estimate of the annual discharge-weighted solute fluxes and alkalinity budgets for the Narayani. The annual fluxes are calculated by using annual discharge-weighted mean (AWM) end-member values in equations (3)–(6). The AWM values are derived by one of two methods. A number of rivers and tributaries in the study area have been sampled during both the monsoon and dry season. The Trisuli river was sampled bi-weekly through the monsoon season at Betrawati barrage [*Galy and France-Lanord*, 1999] providing a robust sample set for our annual flux estimates. For the other rivers in our database that do not have the same frequency of sampling, but do have at least one monsoon sample, we follow the technique of *France-Lanord et al.* [2003] and estimate our annual weighted mean (AWM) using one premonsoon sample, one monsoon sample, and one postmonsoon sample. With this technique, *France-Lanord et al.* [2003] estimated annual weighted mean (AWM) dissolved fluxes for a number of central Nepal streams where one or more monsoon period samples were available. Stream chemical data are weighted by multiyear (5–20) average discharge data (Nepal Department of Hydrology and Meteorology records [*Yogacharya et al.*, 1998] to produce an annual average for each species. The effects of a small sample set were tested by comparing the results based on the full data set from Betrawati (n = 14) with a reduced set containing only 3 samples: one premonsoon, one monsoon, and one postmonsoon sample. The AWM fluxes of the major elements based on the smaller data set were slightly lower than for the full data set, but were all within 15%. The Ge/Si ratio at Betrawati based on a 3-sample limited data set is 3.6 μmol/mol, 17% lower than that based on the full data set (4.3 μmol/mol). The results of this exercise suggest that estimating AWM dissolved fluxes when only 1–3 monsoon period samples is a viable method, producing values within 20% of the true value, biasing Ge/Si ratios to slightly lower values.

8.1. Rivers

[31] At Betrawati, peak discharge normally occurs during August, and is more than an order of magnitude greater than the seasonal low discharge in early spring (Figure 6). Approximately 80% of the annual discharge occurs in the June–September interval. Total dissolved solids drop during the rising limb of the hydrograph from ~110 mg/L to near 60 mg/L, and then recover during the descending limb [*Galy and France-Lanord*, 1999]. Total suspended solids shows considerably greater seasonal variation, with almost all of the sediment transport occurring during the monsoon months. Dissolved silica concentrations fall sharply during the rising limb, increase somewhat through the rest of the monsoon, and return toward higher winter values during the falling limb (Figure 6a). Ge/Si ratios show a similar pattern, though in detail the correlation between Ge/Si and [Si] is not strong (Figure 6b). The AWM Ge/Si ratio of the Trisuli at Betrawati of 4.3 μmol/mol is approximately half of the value observed during the premonsoon season. This value is still considerably elevated with respect to "normal" river values [*Froelich et al.*, 1985] and indicates that the influence of geothermal inputs to the system is significant on an annual, discharge-weighted basis. The high value also suggests that spring discharge increases during the monsoon, although not proportionally to the increase in river discharge. An absolute increase in spring discharge during the monsoon season is consistent with observations of numerous intermittent springs that are dry in the premonsoon but flowing during the monsoon, and local reports that

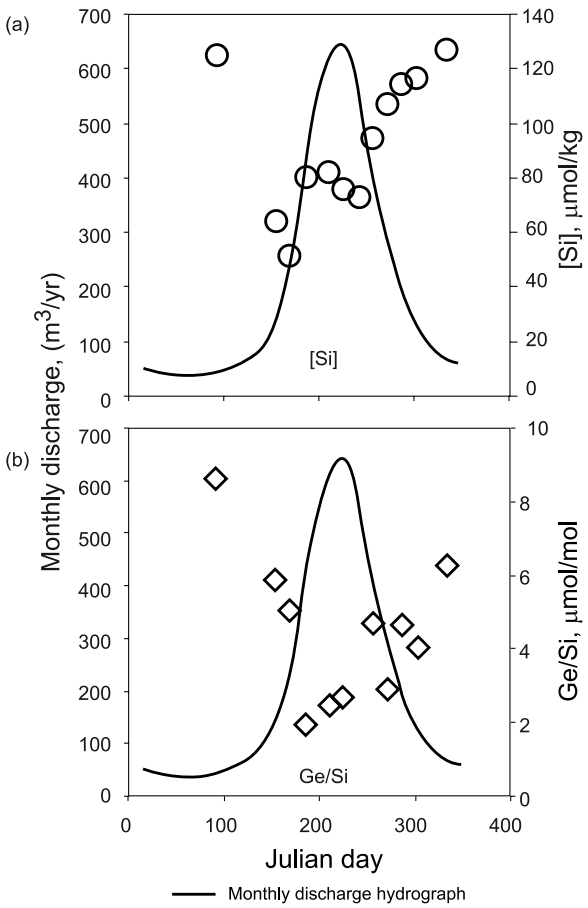

Figure 6. Time series (a) [Si] and (b) Ge/Si versus discharge at Betrawati barrage in the Trisuli River. Discharge (solid line) is shown on the left-hand axis. [Si] and Ge/Si values are on the right-hand axis and are shown as circles and diamonds, respectively. Time shown is approximately 14 months from June 1993 to April 1994. [Si] and Ge/Si decrease with the ~10× monsoon-driven increase in discharge. During the monsoon, [Si] is reduced by approximately a factor of 3 times, Ge/Si by a factor of 2.5. Evidently, hot spring discharge increases during the monsoon but not proportionally to river discharge.

tatopani ("hot spring") flow is much higher during the monsoon.

[32] Ge/Si values and [Cl^-] in the Marsyandi and Trisuli decline by about a factor of 4 during the monsoon, indicating that the fractional hydrothermal input is ~4× higher during the dry season. Estimated AWM values for the mouth of the Marsyandi above its confluence with Trisuli are Ge/Si = 2.2, [Cl^-] = 129 µmol/kg, each about a factor of 2 to 2.5 lower than the premonsoon value. River discharge, however, increases by more than an order of magnitude during the monsoon. Assuming the [Cl^-] and Ge/Si in the hot springs remain constant, this indicates that the fractional contribution from hydrothermal sources declines during the monsoon, but not as much as would be predicted by simple dilution (a factor of 10 or more). Consequently, the absolute spring discharge must increase during the monsoon, on the order of a factor of 2–3.

[33] For the purposes of this study, the AWM river end-member ($(Ge/Si)_R$) was calculated following the procedure of *France-Lanord et al.* [2003] (Table 6). Sufficient data exists for four of the eight rivers in this study to produce AWM $(Ge/Si)_R$ values (the Trisuli, the Marsyandi, the Seti, and the Kali Gandaki). For these rivers, the AWM $(Ge/Si)_R$ is between 1.8 and 2.4 times lower than the dry-season value. As a first-order estimate, we calculated AWM $(Ge/Si)_R$ values for the remaining four rivers using an average reduction of 2.1 times between the dry season and annual value.

8.2. Hot Springs and Tributaries

[34] Monsoon-driven changes in the hot spring and tributary end-members must also be taken into account when using the chemical mass balance to estimate annual solute fluxes. Tributary data is limited; however the Chepe and Darondi Kholas were sampled in both seasons. The available data do not define any clear seasonal differences and consequently, we employ the same tributary end-member for our annual estimate as used above.

[35] Only one hot spring has been sampled during both monsoon and nonmonsoon season. Samples MLB 85 and MO 520 from Tatopani on the Kali Gandaki are close in composition for both major elements and Ge/Si ratio (Figures 7a and 7b). Concentrations of magnesium, calcium, potassium and sulfate are within a few percent, while alkalinity, chloride, fluoride, silica, germanium and sodium are more dilute in the monsoon sample by 12–31%. Ge/Si drops slightly from 93 µmol/mol during the dry season to 85 µmol/mol during the monsoon (Figures 7a and 7b). The Ge-Si systematics of the Nepal hot springs are primarily controlled by quartz solubility, and typically reflect equilibration with quartz at an elevated subsurface temperature [*Evans and Derry*, 2002]. Given this control, unless the flow path of water through the hydrothermal system changes substantially, it is unlikely that the Ge-Si relations of the fluids will change much other than by dilution during seasonal changes in hydrologic fluxes. The limited data above are consistent with this expectation, and so we also

Table 6. Annual F_W^{HS} and Q_{HS} Values Found Using Equation (1)[a]

	Q_R, m^3/s	$[Si]_R$, μmol/kg	$(Ge/Si)_R$, μmol/mol	(n)	$[Si]_{HS}$	$(Ge/Si)_{HS}$	Hot Spring Sample(s)	F_W^{HS}, %	Q_{HS}, m^3/s
Myagdi	195	86	6.1	[b]	584	795	MLB 66, 68, 70, 71	0.18	0.36
Kali	282	87	2.4	3	607	100	MLB 81, 82, 83, 84, 85	0.44	1.25
Modi	26	74	1.5	[b]	517	21	MLB 87, 92	1.24	0.33
Seti	105	99	1.5	3	966	267	MLB 101, 102	0.05	0.05
Marsyandi	210	149	2.2	3	1306	131	MLB 51, 55, 58	0.14	0.29
Bhuri	159	93	0.9	[b]	977	129	GA 217	0.02	0.04
Trisuli	184	124	4.3	13	2053	80	MLB 27, 28, 4, 5	0.36	0.66
Langtang	25	125	1.6	[b]	832	583	MLB 41	0.03	0.01
Sum	1,186							0.25[c]	3

[a] For the annual calculation, the $[Si]_R$ and $(Ge/Si)_R$ in Table 6 were used in combination with $[Si]_{trib}$ = 155 μmol/kg and $(Ge/Si)_{trib}$ = 0.7 μmol/mol. $[Si]_{HS}$ and $(Ge/Si)_{HS}$ values are the same as those in Table 3 (see text).
[b] AWM $(Ge/Si)_R$ values are an average of 2.1 times lower that the dry-season $(Ge/Si)_R$ values. $(Ge/Si)_R$ values for these streams are calculated by dividing the dry-season $(Ge/Si)_R$ by 2.1.
[c] F_W^{HS} for the Narayani system (from sum of 8 rivers).

keep the hydrothermal end-member constant for the monsoon calculation. Clearly more monsoon season data for both streams and hot springs are needed to test these assumptions, but the available data suggests that they are reasonable as a first approximation.

8.3. Annual Flux Estimates

[36] The discharge-weighted annual F_W^{HS} values for the central Nepal rivers based on the above assumptions are presented in Table 6. The results show that on an annual flow basis, the hot spring discharge is between 0.02% and 1.2% of the river discharge. This results in mean annual hot spring discharge values of between 0.01 and 1.3 m^3/s. The AWM value of F_W^{HS} across the Narayani basin is 0.25%, equivalent to a total hot spring discharge ≈3 m^3/s. The fractional contribution is reduced by a factor of 2 relative to that calculated for the premonsoon season, while the absolute flux increases by ~50%.

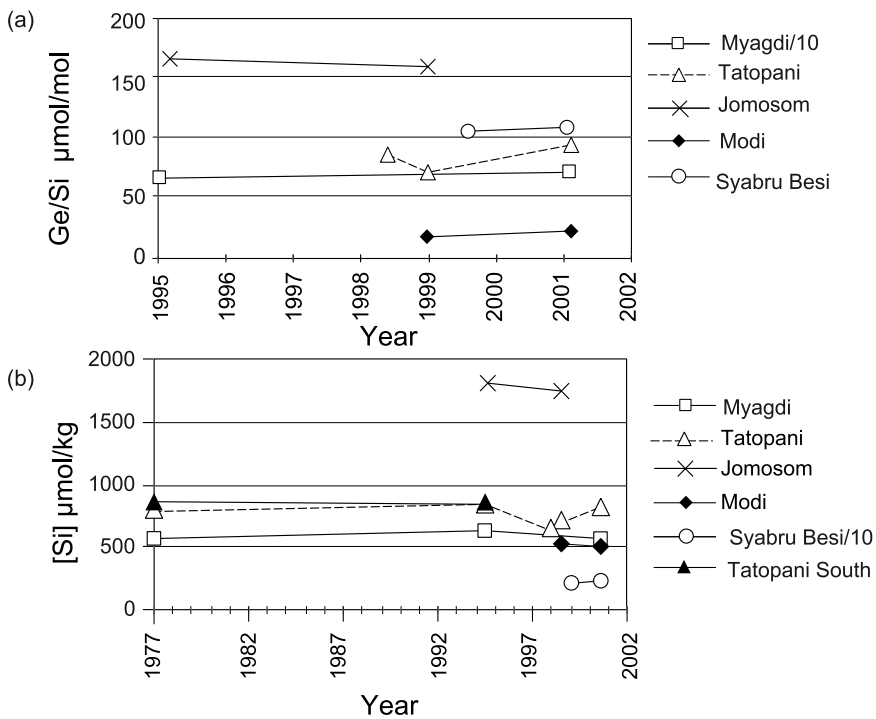

Figure 7. Time series (a) [Si] and (b) Ge/Si for select hot springs in the Myagdi Khola, Modi Khola, Kali Gandaki, and Trisuli river systems. Si concentrations show an average 7% variation over nearly 30 years, and the Ge/Si values vary by 17% over a shorter 6-year span. The consistency in hot spring chemistry probably reflects quartz precipitation control over Si and Ge concentrations. Data are from Table 2 and *Kotarba et al.* [1982].

Table 7. Annual $X\,(ALK^{HS}_{sil})$ Values for Streams of the Narayani Basin

	Q_R, m^3/s	1.25Na** + 1.67K*, μmol/kg	$J(ALK^{R}_{sil})_{annual}$, mol/s	Q_{HS}, m^3/s	1.25Na** + 1.67K*, mol/kg	$J(ALK^{HS}_{sil})_{annual}$, mol/s	$X(ALK^{HS}_{sil})$, %
Myagdi	195	195	38	0.36	16	5.5	15 ± 9
Kali	282	160	45	1.25	2	2.9	7 ± 6
Modi	26	97	2.6	0.33	2	0.8	30 ± 13
Seti	105	166	17	0.05	47	2.4	14 ± 8
Marsyandi	210	143	30	0.29	12	3.5	12 ± 12
Bhuri	159	110	17	0.04	19	0.7	4 ± 3
Trisuli	184	129	24	0.66	13	8.5	36 ± 36
Langtang	25	87	2.1	0.01	5	0.04	2 ± 1
Sum	1186		177	3.0	116	24.4	**14**
Narayani	1601	166	265				**9**

Using the above F^{HS}_{W} values in conjunction with AWM concentrations for ALK, Na**, and K* we can estimate the annual hot spring contribution to the silicate alkalinity budget for the individual rivers and the Narayani as a whole ($J^{HS}_{sil\text{-}annual}$) (Table 7). Again, sufficient data exists only for the Seti, the Marsyandi, the Kali Gandaki and the Trisuli rivers. The AWM ALK, Na**, and K* for these rivers were compared to the dry season values to compute a dry-season/monsoon factor and as with the AWM Ge/Si, this factor was applied to the dry season data for the other four rivers, to estimate the missing AWM alkalinity data.

[37] On an annual basis, the hot springs provide between 2% and 36% of the silicate alkalinity to the individual rivers of the Narayani basin (Table 7), less than during the dry season (Table 5). While their relative contributions are different than during the dry season, four rivers again comprise most (79%) of the hydrothermal flux, the Trisuli, Myagdi, Kali, and Marsyandi. The overall influence of hydrothermal fluxes decreases during the high discharge monsoon season, but this shift in relative importance could simply be a function of our estimation technique. As with the premonsoon season, we estimated the overall impact on the Narayani alkalinity budget by computing the weighted sum of the individual river basins, and by using monsoon season alkalinity data from Narayanigat. Both estimates agree to within error, with the estimate of the hydrothermal portion of the annual silicate alkalinity flux, $(X\,(ALK^{HS}_{sil}))$ between 9 and 13% of the total annual silicate alkalinity flux of the Narayani, a flux of $\approx 7.6 \times 10^8$ eq y^{-1}. We emphasize this is a preliminary estimate, and likely to be biased toward low values for two reasons. First, in assigning hot spring chloride to a halite and/or cyclic origin, we have probably underestimated the Na from silicate sources in some springs. Second, the precipitation of hydrothermal carbonate removes Ca^{2+} and alkalinity from solution. However, these deposits are later eroded and dissolved, and appear in stream waters as products of carbonate dissolution, despite the fact that a significant portion originated as silicate alteration products. Essentially, dissolution of hydrothermal carbonate adds silicate-derived alkalinity to stream waters in a two step process. Ca^{2+} is released by silicate alteration in hydrothermal systems, neutralizing carbonic acid and generating alkalinity. Precipitation removes these components, but later weathering will reintroduce them to the hydrologic system. Only after the precipitated hydrothermal carbonate is redissolved does the alkalinity generated by hydrothermal silicate alteration become part of the stream budget, and it does so with all the appearances of carbonate dissolution. We do not here attempt to quantify the flux of silicate alkalinity that passes through this two step process, with a time delay dependent on the rate of erosion and weathering of hydrothermal carbonate deposits. However a simple consideration of the amount of carbonate precipitated in a carbonate saturated hydrothermal system as fluids rise to the surface suggests that this flux could easily be at least equal in magnitude to the observed dissolved alkalinity flux in the springs.

9. Conclusions

[38] Hot springs located near major structural and topographic breaks in central Nepal make a significant contribution to the solute load of large streams. Hot spring fluid chemistry primarily reflects silicate alteration, while river chemistry upstream of geothermal zones is primarily dominated by carbonate dissolution. Germanium-silicon systematics are a

useful quantitative tracer of hydrothermal fluid input, as this ratio is very high in hydrothermal fluids in almost all settings, but low in normal stream environments. We used the Ge/Si mass balance to estimate the fractional contribution of geothermal systems to the river water flux, and to the river alkalinity. We find that during the premonsoon season geothermal fluids account for 0.5 ± 0.3% of the water flux and 25 ± 15% of the silicate alkalinity flux. Combining these results with discharge measurements, we estimate that the hydrothermal water discharge is 2.0 m^3/s with a factor of 2 uncertainty and the alkalinity flux is 20 ± 14 moles/s across the entire Narayani river basin. Thus a small fraction of hydrothermal water input has a large effect on the silicate alkalinity flux, and contributes a significant fraction of the total.

[39] Sufficient data are not yet available to make an equivalent estimate of the hydrothermal flux on an annual basis, because of the very large seasonal variations in water flux and smaller but important variations in solute chemistry. We have made a preliminary estimate of the importance of hydrothermal sources to the annual flux budgets of water and silicate derived alkalinity using interpolations of existing data. It appears that the fractional contribution of hydrothermal sources to the water and silicate alkalinity budgets are about a factor of three to five lower during the monsoon (depending on the individual river system), implying a relative contribution weighted over the annual cycle of ~2.5 × less than we calculated for the premonsoon season. If this estimate is near correct, hydrothermal sources would account for approximately 10% of the silicate alkalinity carried by the Narayani river system through the year.

[40] An additional source of silicate derived alkalinity that we have identified but not quantified here is the dissolution of hydrothermal carbonate during later erosion and weathering of fossil hydrothermal systems. Ca and Mg are released during hydrothermal alteration of silicate rocks, and an unknown but potentially considerable fraction is precipitated as carbonate within the silicate host rock. Later weathering of this carbonate will yield solute features that are difficult to distinguish from dissolution of sedimentary carbonate. Weathering of hydrothermal carbonate releases alkalinity that was originally derived from silicate alteration. While the importance of trace carbonate dissolution to the solute flux from silicate has been established in the Himalaya and elsewhere, its role in the overall silicate-carbonate cycle has been overlooked.

Notation

Q_R	main stem discharge downstream of hydrothermal flows.
Q_{HS}	hot spring discharge.
Q_{trib}	all surface water discharge upstream of and unaffected by hydrothermal flows.
Na*	$[Na^+] - [Cl^-]$.
Na**	$[Na^+] - [Cl^-] - [Na^+]$ from atmospheric deposition.
K*	$[K^+] - [K^+]$ from atmospheric deposition.
F_W^{HS}	fraction of the total river discharge contributed by the hot springs.
$[ALK]_{sil}$	silicate alkalinity in general, defined in equation (4) as Na** + K^+.
$[ALK]_T^{HS}$	total hot spring alkalinity.
F_{sil}^{HS}	fraction of the total hot spring alkalinity derived from silicate sources.
$[ALK]_T^R$	total riverine alkalinity.
$[ALK]_{sil}^R$	total riverine silicate alkalinity.
F_{sil}^R	fraction of the total river alkalinity derived from silicate sources.
$X(ALK_{sil}^{HS})$	fraction of the total riverine silicate alkalinity contributed by the hot springs.
$J(ALK_{sil}^R)$	riverine silicate alkalinity flux.
$J(ALK_{sil}^{HS})$	hot spring silicate alkalinity flux.
$J(ALK_{sil}^{HS})_{annual}$	annual hot spring silicate alkalinity flux.
$J(ALK_{sil}^R)_{annual}$	annual riverine silicate alkalinity flux.

Acknowledgments

[41] A number of individuals contributed to the field work and resultant sample set used here, in particular Albert Galy, Ananta Gajurel, Suzanne Anderson, Bob Darling and Jean Riotte. This work was supported by NSF grant EAR 0087671, by the CNRS, and by the Cornell Program in Biogeochemistry.

References

Anders, A. M., R. S. Sletten, L. A. Derry, and B. Hallet (2003), Germanium/silicon ratios in the Copper River Basin, Alaska: Weathering and partitioning in periglacial versus glacial environments, *J. Geophys. Res.*, *108*(F1), 6005, doi:10.1029/2003JF000026.

Arnorsson, S. (1984), Germanium in Icelandic geothermal systems, *Geochim. Cosmochim. Acta*, *48*, 2489–2502.

Bhattarai, D. R. (1980), Some geothermal springs of Nepal, *Tectonophysics*, *62*, 7–11.

Burchfiel, B. C., and L. H. Royden (1985), North-south extension within the convergent Himalayan region, *Geology*, *13*(10), 679–682.

Burg, J. P., M. Brunel, D. Gapais, G. M. Chen, and G. H. Liu (1984), Deformation of leucogranites of the crystalline Main Central Sheet in Southern Tibet (China), *J. Struct. Geol.*, *6*(5), 535–542.

Chillrud, S. N., F. L. Pedrozo, P. F. Temporetti, H. F. Planas, and P. N. Froelich (1994), Chemical-weathering of phosphate and germanium in glacial meltwater streams—Effects of subglacial pyrite oxidation, *Limnol. Oceanogr.*, *39*(5), 1130–1140.

Colchen, M., P. Le Fort, and A. Pêcher (1986), Notice explicative de la carte géologique Annapurna-Manaslu-Ganesh (Himalaya du Népal) au 1:200.000e (bilingue: Français-English), Cent. Natl. de la Rech. Sci., Paris.

Criaud, A., and C. Fouillac (1986), Study of CO_2-rich thermomineral waters from the Central French Massif. 2. Behavior of some trace-metals, arsenic, antimony and germanium, *Geochim. Cosmochim. Acta*, *50*(8), 1573–1582.

Dalai, T. K., S. Krishnaswami, and M. M. Sarin (2002), Major ion chemistry in the headwaters of the Yamuna river system: Chemical weathering, its temperature dependence and CO_2 consumption in the Himalaya, *Geochim. Cosmochim. Acta*, *66*(19), 3397–3416.

Derry, L. A., and C. France-Lanord (1997), Himalayan weathering and erosion fluxes: Climate and tectonic controls, in *Tectonic Uplift and Climate Change*, edited by W. F. Ruddiman, pp. 269–312, Plenum, New York.

Dowling, C. B., R. J. Poreda, and A. R. Basu (2003), The groundwater geochemistry of the Bengal Basin: Weathering, chemsorption, and trace metal flux to the oceans, *Geochim. Cosmochim. Acta*, *67*(12), 2117–2136.

English, N. B., J. Quade, P. G. DeCelles, and C. N. Garzione (2000), Geologic control of Sr and major element chemistry in Himalayan Rivers, Nepal, *Geochim. Cosmochim. Acta*, *64*(15), 2549–2566.

Evans, M. J., and L. A. Derry (2002), Quartz control of high germanium/silicon ratios in geothermal waters, *Geology*, *30*(11), 1019–1022.

Evans, M. J., L. A. Derry, S. P. Anderson, and C. France-Lanord (2001), Hydrothermal source of radiogenic Sr to Himalayan rivers, *Geology*, *29*(9), 803–806.

France-Lanord, C., and L. A. Derry (1997), Organic carbon burial forcing of the carbon cycle from Himalayan erosion, *Nature*, *390*(6655), 65–67.

France-Lanord, C., L. Derry, and A. Michard (1993), Evolution of the Himalaya since Miocene time: Isotopic and sedimentologic evidence from the Bengal Fan, in *Himalayan Tectonics*, edited by P. J. Treloar and M. Searle, *Geol. Soc. Spec. Publ.*, *74*, 603–621.

France-Lanord, C., M. Evans, J. Hurtrez, and J. Riotte (2003), Annual dissolved fluxes from Central Nepal rivers: Budget of chemical erosion in the Himalayas, *C. R. Geosci.*, *335*(16), 1131–1140.

Froelich, P. N., G. A. Hambrick, M. O. Andreae, R. A. Mortlock, and J. M. Edmond (1985), The geochemistry of inorganic germanium in natural waters, *J. Geophys. Res.*, *90*, 1133–1141.

Froelich, P. N. V., R. A. Blanc, R. A. Mortlock, S. N. Chillrud, W. Dunstan, A. Udomkit, and T.-H. Peng (1992), River fluxes of dissolved silica to the ocean were higher during glacials: Ge/Si in diatoms, rivers, and oceans, *Paleoceanography*, *7*(6), 739–767.

Galy, A., and C. France-Lanord (1999), Weathering processes in the Ganges-Brahmaputra basin and the riverine alkalinity budget, *Chem. Geol.*, *159*(1–4), 31–60.

Hemming, N. G., and G. N. Hanson (1992), Boron isotopic composition and concentration in modern marine carbonates, *Geochim. Cosmochim. Acta*, *56*(1), 537–543.

Herschy, R. W. (1995), *Streamflow Measurement*, 524 pp., Routledge, New York.

Hodges, K. V., R. R. Parrish, T. B. Housh, D. R. Lux, B. C. Burchfiel, L. H. Royden, and Z. Chen (1992), Simultaneous Miocene extension and shortening in the Himalayan orogen, *Science*, *258*(5087), 1466–1470.

Hurtrez, J. E. (1998), Analyse geomorphologique des interactions Tectonique-Erosion dans le systeme Himalayen, Ph.D. thesis, Institut des Sciences de la Terre, de l'Environnement et de l'Espace de Montpellier, Univ. Montpellier 2, Montpellier, France.

Jacobson, A. D., and J. D. Blum (2000), Ca/Sr and $^{87}Sr/^{86}Sr$ geochemistry of disseminated calcite in Himalayan silicate rocks from Nanga Parbat: Influence on river-water chemistry, *Geology*, *28*(5), 463–466.

Jacobson, A. D., J. D. Blum, C. P. Chamberlain, D. Craw, and P. O. Koons (2003), Climatic and tectonic controls on chemical weathering in the New Zealand Southern Alps, *Geochim. Cosmochim. Acta*, *67*(1), 29–46.

Jamieson, R. A., C. Beaumont, M. H. Nguyen, and B. Lee (2002), Interaction of metamorphism, deformation and exhumation in large convergent orogens, *J. Metamorph. Geol.*, *20*(1), 9–24.

Kilpatrick, F. A., and E. D. Cobb (1985), Measurement of discharge using tracers, in *Techniques of Water-Resources Investigations of the U.S. Geological Survey*, vol. 3, chap. A16, pp. 1–49, U.S. Geol. Surv., Denver, Colo.

Kotarba, M., A. Sokolowski, and W. Bogacz (1982), Hydrogeological investigation in the Kali Gandaki thermal springs area (Nepal Himalayas), *Bull. Acad. Pol. Sci. Ser. Sci. Terre*, *29*(4), 283–291.

Krishnaswami, S., J. R. Trivedi, M. M. Sarin, R. Ramesh, and K. K. Sharma (1992), Strontium isotopes and rubidium in the Ganga-Brahmaputra river system: Weathering in the Himalaya, fluxes to the Bay of Bengal and contributions to the evolution of oceanic $^{87}Sr/^{86}Sr$, *Earth Planet. Sci. Lett.*, *109*, 243–253.

Ku, H. H. (1969), Statistical concepts in metrology, in *Precision Measurement and Calibration*, edited by H. H. Ku, pp. 296–330, Natl. Bur. of Stand., Washington, D. C.

Kurtz, A. (2000), Germanium/silicon and trace element geochemistry of silicate weathering and mineral aerosol deposition, Ph.D. thesis, Cornell Univ., Ithaca, N. Y.

Kurtz, A., L. A. Derry, and O. A. Chadwick (2002), Germanium-silicon fractionation in the weathering environment, *Geochim. Cosmochim. Acta*, *66*(9), 1525–1537.

Lave, J., and J. P. Avouac (2001), Fluvial incision and tectonic uplift across the Himalayas of central Nepal, *J. Geophys. Res.*, *106*(B11), 26,561–26,591.

Le Fort, P. (1975), Himalaya: The collided range. Present knowledge of the continental arc, *Am. J. Sci.*, *275*(A), 1–44.

Mortlock, R. A., and P. N. Froelich (1987), Continental weathering of germanium—Ge/Si in the global river discharge, *Geochim. Cosmochim. Acta*, *51*(8), 2075–2082.

Mortlock, R. A., and P. N. Froelich (1996), Determination of germanium by isotope dilution hydride generation inductively coupled plasma mass spectrometry, *Anal. Chim. Acta*, *332*(2–3), 277–284.

Mortlock, R. A., P. N. Froelich, R. A. Feely, G. J. Massoth, D. A. Butterfield, and J. E. Lupton (1993), Silica and germanium in Pacific Ocean hydrothermal vents and plumes, *Earth Planet. Sci. Lett.*, *119*(3), 365–378.

Murnane, R. J., and R. F. Stallard (1990), Germanium and silicon in rivers of the Orinoco drainage basin, *Nature*, *344*(6268), 749–752.

Pande, K., M. M. Sarin, J. R. Trivedi, S. Krishnaswami, and K. K. Sharma (1994), The Indus River System (India-Pakistan)—Major-ion chemistry, uranium and strontium isotopes, *Chem. Geol.*, *116*(3–4), 245–259.

Parrish, R. R., and K. V. Hodges (1996), Isotopic constraints on the age and provenance of the Lesser and Greater Himalayan sequences, Nepalese Himalaya, *Geol. Soc. Am. Bull.*, *108*(7), 904–911.

Quade, J., L. Roe, P. G. DeCelles, and T. P. Ojha (1997), The late Neogene $^{87}Sr/^{86}Sr$ record of lowland Himalayan rivers, *Science*, *276*(5320), 1828–1831.

Rybach, L. (1981), Geothermal systems, conductive heat flow, geothermal anomalies, in *Geothermal Systems: Principles and Case Histories*, edited by L. Rybach and J. L. P. Muffler, pp. 3–36, John Wiley, Hoboken, N. J.

Sai-Halasz, C. (1999), Geomorphology of erosional regimes in the Himalayas, M.S. thesis, Cornell Univ., Ithaca, N. Y.

Sarin, M. M., S. Krishnaswami, K. Dilli, B. l. K. Omayajulu, and W. S. Moore (1989), Major ion chemistry of the Ganga-Brahmaputra river system: Weathering processes and fluxes to the Bay of Bengal., *Geochim. Cosmochim. Acta*, *53*, 997–1009.

Sarin, M. M., S. Krishnaswami, J. R. Trivedi, and K. K. Sharma (1992), Major ion chemistry of the Ganga source waters—Weathering in the high-altitude Himalaya, *Proc. Indian Acad. Sci. Earth Planet. Sci.*, *101*(1), 89–98.

Seeber, L., and V. Gornitz (1983), River profiles along the Himalayan Arc as indicators of active tectonics, *Tectonophysics*, *92*(4), 335–367.

Singh, S. K., J. R. Trivedi, K. Pande, R. Ramesh, and S. Krishnaswami (1998), Chemical and strontium, oxygen, and carbon isotopic compositions of carbonates from the Lesser Himalaya: Implications to the strontium isotope composition of the source waters of the Ganga, Ghaghara, and the Indus rivers, *Geochim. Cosmochim. Acta*, *62*(5), 743–755.

Stallard, R. F., and J. M. Edmond (1981), Geochemistry of the Amazon: 1. Precipitation chemistry and the marine contribution to the dissolved-load at the time of peak discharge, *J. Geophys. Res.*, *86*, 9844–9858.

West, A. J., M. J. Bickle, R. Collins, and J. Brasington (2002), Small-catchment perspective on Himalayan weathering fluxes, *Geology*, *30*(4), 355–358.

Wobus, C. W., K. V. Hodges, and K. X. Whipple (2003), Has focused denudation sustained active thrusting at the Himalayan topographic front?, *Geology*, *31*(10), 861–864.

Yogacharya, K. S., A. P. Pokhrel, and S. R. Kansakar (1998), *Hydrological Records of Nepal: Streamflow Summary*, 264 pp., Dep. of Hydrol. and Meteorol., H. M. G. of Nepal Minist. of Sci. and Technol., Kathmandu, Nepal.